

PAPER

# Silicon drift detectors system for high-precision light kaonic atoms spectroscopy

To cite this article: M Miliucci *et al* 2021 *Meas. Sci. Technol.* **32** 095501

View the [article online](#) for updates and enhancements.

# Silicon drift detectors system for high-precision light kaonic atoms spectroscopy

M Miliucci<sup>1,\*</sup> , A Scordo<sup>1,\*</sup>, D Sirghi<sup>1,2,\*</sup>, A Amirkhani<sup>3</sup>, A Baniahmad<sup>3</sup>, M Bazzi<sup>1</sup>, D Bosnar<sup>4</sup> , M Bragadireanu<sup>2</sup>, M Carminati<sup>3</sup>, M Cargnelli<sup>5</sup>, A Clozza<sup>1</sup>, C Curceanu<sup>1</sup>, L De Paolis<sup>1</sup>, R Del Grande<sup>1,6,7</sup> , C Fiorini<sup>3</sup>, C Guaraldo<sup>1</sup>, M Iliescu<sup>1</sup>, M Iwasaki<sup>8</sup>, P Levi Sandri<sup>1</sup>, J Marton<sup>5</sup>, P Moskal<sup>9</sup>, F Napolitano<sup>1</sup>, S Niedźwiecki<sup>9</sup>, K Piscicchia<sup>1,7</sup>, F Sgaramella<sup>1,10</sup>, H Shi<sup>1,5</sup>, M Silarski<sup>9</sup>, F Sirghi<sup>1,2</sup>, M Skurzok<sup>1,9</sup>, A Spallone<sup>1</sup>, M Tüchler<sup>5</sup>, O Vazquez Doce<sup>1,6</sup> and J Zmeskal<sup>5</sup>

<sup>1</sup> INFN-LNF, Istituto Nazionale di Fisica Nucleare—Laboratori Nazionali di Frascati, Frascati (Roma), Italy

<sup>2</sup> Horia Hulubei National Institute of Physics and Nuclear Engineering (IFIN-HH), Magurele, Romania

<sup>3</sup> Politecnico di Milano, Dipartimento di Elettronica, Informazione e Bioingegneria and INFN Sezione di Milano, Milano, Italy

<sup>4</sup> Department of Physics, Faculty of Science, University of Zagreb, Zagreb, Croatia

<sup>5</sup> Stefan-Meyer-Institut für Subatomare Physik, Vienna, Austria

<sup>6</sup> Excellence Cluster Universe, Technische Universität München, Garching, Germany

<sup>7</sup> Centro Ricerche Enrico Fermi—Museo Storico della Fisica e Centro Studi e Ricerche ‘Enrico Fermi’, Roma, Italy

<sup>8</sup> RIKEN, Tokyo, Japan

<sup>9</sup> M. Smoluchowski Institute of Physics, Jagiellonian University, Kraków, Poland

<sup>10</sup> Università degli Studi di Roma, Tor Vergata, Rome, Italy

E-mail: [Marco.Miliucci@lnf.infn.it](mailto:Marco.Miliucci@lnf.infn.it), [Alessandro.Scordo@lnf.infn.it](mailto:Alessandro.Scordo@lnf.infn.it) and [Diana.Laura.Sirghi@lnf.infn.it](mailto:Diana.Laura.Sirghi@lnf.infn.it)

Received 22 December 2020, revised 9 March 2021

Accepted for publication 15 March 2021

Published 26 May 2021



CrossMark

## Abstract

A large area silicon drift detectors (SDDs) system and its readout electronics have been developed by the SIDDHARTA-2 Collaboration, aiming to perform high-precision light kaonic atoms x-ray spectroscopy for the investigation of the  $\bar{K}N$  strong interaction in the low-energy QCD regime. To perform these measurements, a linear energy response and a good energy resolution are mandatory requirements for the system, to be preserved along the whole DAQ (analog and digital) chain; such task is made even harder in the experimental environment of particles colliders, where the high background due to ionizing particles and radiation is present. The energy response of the SDDs system has been characterized with the beam-originating background generated during the commissioning phase of the DAΦNE electron–positron collider (INFN-LNF) in early 2020. The data analysis has been optimized to describe the system’s response and the background. The calibration procedure demonstrates that, despite the high and variable background of the collider, the energy response of the system is linear at the level of few eV ( $(\Delta E/E) < 10^{-3}$ ), with an energy resolution of  $157.8 \pm 0.3_{-0.2}^{+0.2}$  eV for the Fe  $K_{\alpha}$  line.

\* Authors to whom any correspondence should be addressed.

Keywords: silicon drift detector, x-ray spectroscopy, kaonic atoms

(Some figures may appear in colour only in the online journal)

## 1. Introduction

Silicon drift detectors (SDDs) are widely used in various fields [1–4] and, thanks to their excellent performances in terms of energy resolution, electronic noise suppression and high rate capability, have also become an instrument used for precision spectroscopy experiments. Among these, a key role is played by SDDs in the light kaonic atoms x-ray spectroscopy [3], where their excellent capabilities are exploited to extract the shift ( $\varepsilon$ ) and the width ( $\Gamma$ ) of the atomic levels caused by the  $\bar{K}N$  strong interaction. These observables are fundamental quantities for the understanding of the non-perturbative QCD (quantum chromodynamics) in the strangeness sector, having implications ranging from particle and nuclear physics to astrophysics [5–8].

The SIDDHARTA experiment [9] employed in 2009, for the first time, a SDDs based system to perform the kaonic hydrogen (K<sup>-</sup>H) x-ray spectroscopy at the DAΦNE collider [10, 11] of Istituto Nazionale di Fisica Nucleare–Laboratori Nazionali di Frascati (INFN–LNF), achieving the most precise measurement of the shift ( $\varepsilon$ ) and the width ( $\Gamma$ ) for the K<sup>-</sup>H fundamental level. Combining this result with the analogous measurement of the kaonic deuterium (K<sup>-</sup>d)  $2p \rightarrow 1s$  transition, to be performed by SIDDHARTA-2 in 2021, it will be possible to extract the isospin dependent antikaon-nucleon scattering lengths, which are fundamental quantities for understanding the low-energy QCD in the strangeness sector. Theoretical calculations [12–14] together with Monte Carlo simulations [7] set the region of interest (ROI) of the SIDDHARTA-2 measurement from 4000 eV to 12 000 eV, making Silicon-based devices the best candidates for x-ray detection thanks to their high quantum efficiency (>85% for 450  $\mu\text{m}$  thick Silicon wafer) and good energy resolution. Furthermore, the one order of magnitude lower yield for the K<sup>-</sup>d  $2p \rightarrow 1s$  transition with respect to the analogous K<sup>-</sup>H [15] demands the development of improved technologies to achieve a precision comparable with the SIDDHARTA one.

The SIDDHARTA-2 collaboration has built an experimental apparatus based on an innovative SDDs system (see section 2 for details) aiming to perform high-precision x-ray spectroscopy measurement of the K<sup>-</sup>d fundamental level. From the Monte Carlo simulation [7], considering the improvement of the SIDDHARTA-2 apparatus with respect to SIDDHARTA, the extracted shift and width can be determined with precision of about 30 and 80 eV, respectively, so the same order as the SIDDHARTA results. To achieve this, a linear energy response, together with a good energy resolution, are mandatory requirements for the SDDs system. Moreover, the main experimental challenge consists in the development of a high-precision spectroscopy system able to operate within the ionizing particles and radiation background generated by the DAΦNE collider. The SIDDHARTA-2 SDDs system has

been tested for the first time at the DAΦNE collider, during the beam commissioning phase in early 2020 and this work presents the results of the data analysis.

A robust fitting function has been defined in order to describe the background and to identify the elements with fluorescence lines detected by the SDDs system. Consequently, a calibration procedure has been employed to evaluate the energy response of the system, resulting in a linearity of  $\Delta E/E < 10^{-3}$  and an energy resolution (FWHM) at the Fe  $K_{\alpha}$  line of  $157.8 \pm 0.3_{-0.2}^{+0.2}$  eV.

## 2. SIDDHARTA-2 experimental apparatus

The SIDDHARTA-2 apparatus (figure 1(a)), consists of an aluminum vacuum chamber of cylindrical shape equipped with a closed cycle Helium refrigerator, which keeps the target cell temperature between 20 K and 30 K and the SDDs, that surround the target, stable around 170 K. Plastic scintillators are placed around the target cell, arranged externally (Veto-1) and internally (Veto-2) with respect to the vacuum chamber, for an efficient rejection of the hadronic background. Additional scintillators systems, working in coincidence mode on the vertical and horizontal plane with respect to the beam pipe, act, respectively, as kaon trigger for the electromagnetic background rejection and luminosity monitor [16]. For the aim of the present work, the upper component of the kaon trigger has been replaced by a x-ray tube equipped with a calibration target, as schematically presented in figure 1(b). The photons emitted by the x-ray source during the beam commissioning phase, hit the SDDs inside the vacuum chamber passing through a 150  $\mu\text{m}$  thick mylar window ( $\phi = 60$  mm). The calibration target, made of Ti, Fe, Cu, Br and Sr strips laid above a 5 mm thick teflon plate to reject the W-lines coming from the cathode, is placed on the top of the x-ray tube Be window. The x-ray tube activates the multi-element target materials and their  $K_{\alpha}$  and  $K_{\beta}$  transitions are detected by the SDDs system, covering an energy range from 4000 eV to 16 000 eV.

### 2.1. SIDDHARTA-2 Silicon Drift Detectors system

The SDDs used by SIDDHARTA-2 consist in a silicon cylindrical  $n^{-}$  bulk, double sided by  $p^{+}$  silicon doped electrodes [17–19]. On the top, a non-structured  $p^{+}$  layer forms the light entrance window. On the opposite side,  $p^{+}$  concentric rings are biased with a negative voltage through an internal divider, which minimizes the connections only to the external and internal rings. Lastly, the  $n^{+}$  small area collecting anode is placed at the center of the structured layer and connected to the dedicated front-end electronic.

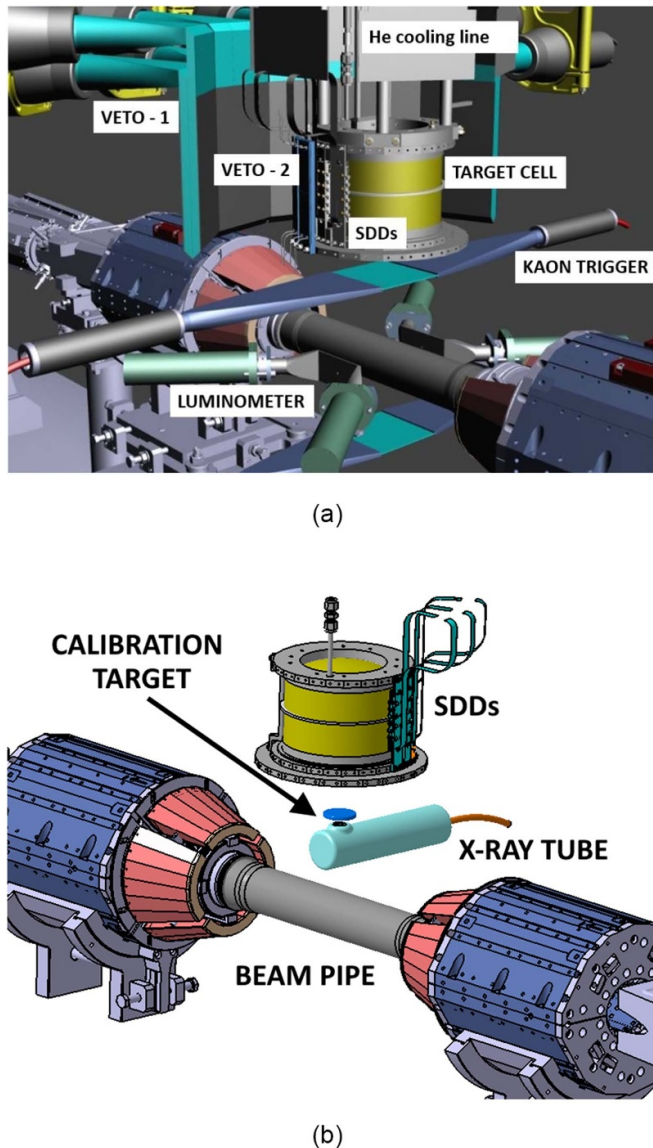


**Figure 1.** (a) Schematic view of the SIDDHARTA-2 setup. (b) Illustration of the calibration configuration (not in scale).

New monolithic SDDs arrays (figure 2) have been developed by Fondazione Bruno Kessler, Politecnico di Milano, INFN-LNF (Italy) and the Stefan Meyer Institute (Austria) to perform high-precision light kaonic atoms spectroscopy. The 450  $\mu\text{m}$  thick SDDs array is composed by eight separated SDD units (0.64  $\text{cm}^2$  area for each single cell) organized in a  $2 \times 4$  matrix for a total active area of 5.12  $\text{cm}^2$  (active/total surface ratio of 0.75). The large area SDDs system for the SIDDHARTA-2 experiment consists of an SDDs array glued on an alumina carrier for the SDD units polarization and coupled to the dedicated front-end electronics for the x-ray signal processing.

The device is screwed on a high purity aluminum support which provides the cooling power to reduce the electronic noise due to the leakage current of the SDD units, thus improving their energy resolution. The structure of the ceramic carrier (gear-wheel type) allows a close packaging of

the SDDs arrays around the target cell, optimizing the geometrical efficiency. The SDDs are supplied by an external voltage which has been previously optimized during the preliminary laboratory tests [20]. A CMOS low-noise charge sensitive preamplifier (CUBE) [21] is mounted on the alumina carrier and bonded to the  $n^+$  anode, for each single cell. The CUBE preamplifier, installed close to the SDD anode, has been designed to render the device's performance independent from the applied bias voltages and to increase its stability, even when exposed to high charged particle rates generated by the collider operations. Furthermore, this solution allows to operate at lower cryogenic temperature with respect to an external J-FET preamplification stage, thus obtaining an electronic noise systematically lower. The detectors are coupled to a dedicated ASIC (SDDs Front-End Readout ASIC, SFERA) [22, 23], including fast and slow shapers with programmable parameters in order to improve the spectroscopic response of the system. Each SFERA chip, after processing the signals coming from two SDDs arrays, provides the amplitude and the timing information of the detected event.

The block diagram in figure 3 shows the signal processing chain of the SIDDHARTA-2 SDDs system unit, for the *Kaonic Deuterium high-precision x-ray spectroscopy*. The single cell capacitor ( $C_0$ ) is charged both by the leakage current and the electron packets produced by the absorbed radiation, while the charge collection at the SDD anode is represented as a current pulse ( $Q_0$ ).

It follows that the output of the CUBE, whose gain is set for an energy range from few hundreds eV to 20 000 eV, consists of steps generated by the charge collection to the anode, over-imposed on a slow rising ramp due to the leakage current of the detector. The signal related to the x-ray event is separated from the leakage current through a robust filtering stage with shaping time of 2  $\mu\text{s}$  to minimize the noise contribution. Then, the maximum value of the Gaussian output of the main shaper is held by the peak stretcher (PKS) circuit. The hit-activated channels are put at disposal, on DAQ request, of the multiplexer output, from where the voltage is converted into digital format by an analog-to-digital converter (ADC, model NI-PCI 6115). Finally, a National Instrument package, including a Multi Channel Analyzer, handles the ADCs and the external logic, storing the full event data information.

The signal processing chain robustness, expressed in terms of linear energy response and low electronic noise, plays a crucial role in achieving high-precision x-ray spectroscopy measurements. The energy response of the SDDs system developed by the SIDDHARTA-2 Collaboration for the precise measurement of the ( $K^-d$ ) fundamental level has been evaluated within the ionizing particles and radiation background induced by DAΦNE collider during beam commissioning phase.

### 3. Silicon drift detectors system's energy response

In early 2020 the DAΦNE operations were devoted to the optimization of the beams optics, which caused the SDDs exposure to the ionizing radiations generated by the beams

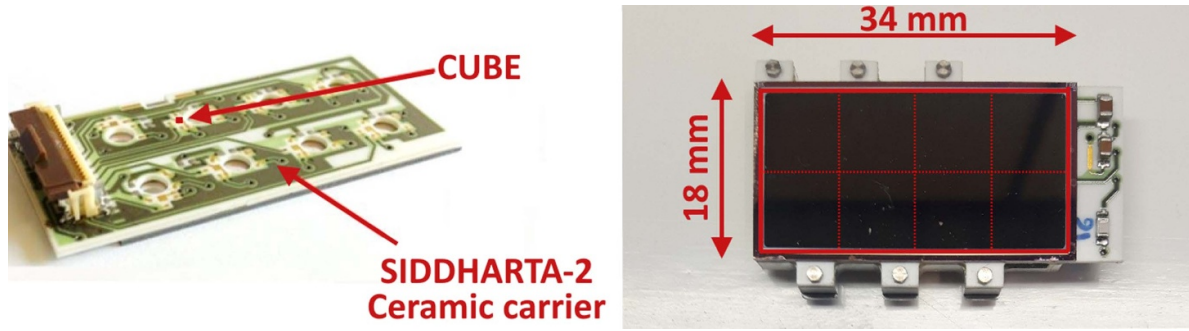


**Figure 2.** Left: The SIDDHARTA-2 ceramic carrier which provides a common polarization to the single cells and amplifies the collected signal through CUBE. Right: Picture of the SIDDHARTA-two silicon drift detectors  $2 \times 4$  array screwed on the aluminium block. The red rectangle defines the active area of the device ( $5.12 \text{ cm}^2$ ) given by the eight cells of  $0.64 \text{ cm}^2$  each.

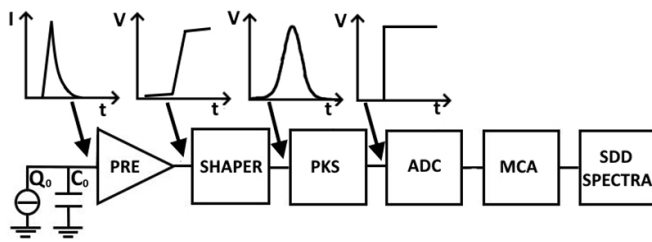


**Figure 3.** Schematic representation of the SDDs readout system. On top, representation of the signal shape for an x-ray event detected by the SDDs system unit.

showering effects in the mechanical elements of the machine and experimental setup. This environment offered the opportunity to test for the first time the SDDs systems in a more stressful and realistic environment than typical laboratory tests.

The peak energy response of the SDDs can be expressed as a Gaussian distribution with a low energy tail due to the incomplete charge collection. We used the accurate models in [24–26] to define the fitting function for the final shape of the peaks and each fluorescence x-ray contains the following two components:

$$G(x) = H_G \cdot e^{-\frac{(x-x_0)^2}{2\sigma^2}} \quad (1)$$

$$T(x) = \frac{H_T}{2\beta\sigma} \cdot e^{\frac{x-x_0}{\beta\sigma} + \frac{1}{2\beta^2}} \cdot \operatorname{erfc}\left(\frac{x-x_0}{\sqrt{2}\sigma} + \frac{1}{\sqrt{2}\beta}\right) \quad (2)$$

where the Gauss function  $G(x)$  represents the fluorescence x-rays and the tail  $T(x)$  represents the events with charge-loss inside the unit.  $H_G$  and  $H_T$  are, respectively, the height of the Gaussian and of the tail,  $\sigma$  defines the resolution for each Gaussian peak and  $\beta$  is the slope of the tail. The shape of the background is represented by the linear combination of a first-grade polynomial and an exponential function.

Figure 4 reports, as an example, the case-study of the energy response for a SDDs system unit. For the purpose of this work we focused on the energy range from 4000 eV to 16 000 eV, widely including the SIDDHARTA-2 ROI [7].

For each calibration element the  $K_\alpha$  fluorescent line (higher S/N ratio) has been selected, maximizing the precision for the linear response evaluation. To interpolate the calibration points, whose coordinates are the theoretical ( $P_i^{\text{label}}$ ) and the experimental ( $P_i^{\text{exp}}$ ) energy values of each single  $K_\alpha$  peak, a first-grade polynomial function has been used (see figure 4 top-right), with the slope of the function representing the system ADC-to-eV gain. The final calibrated spectrum is shown in figure 4 bottom-left.

The linearity evaluation was established through the calculation of the residuals ( $R_i$ ), which are given by the difference between each single calibrated point ( $P_i^{\text{cal}}$ ) and the theoretical ( $P_i^{\text{label}}$ ) value:

$$R_i = P_i^{\text{label}} - P_i^{\text{cal}}. \quad (3)$$

The residuals plot in figure 4 bottom-right reveals an uncorrelated distribution around zero which differs only few eV from the perfect linear case, setting the linear response  $\Delta E/E$  of the investigated SDDs system unit below  $10^{-3}$ .

The systematic errors are evaluated by applying, with respect to the reference fit, a different binning to the spectrum (no rebinning and double binning width with respect to the four time bin width channels of the reference fit) or using only a first grade polynomial to describe the background, removing the exponential contribution. Table 1 lists the residual values obtained for the SDDs system unit of figure 4 and the systematic errors corresponding to their maximum deviation. The amplitudes of the systematic errors are at least one order of magnitude lower with respect to the statistical ones, thus the effect induced by the fitting procedure to the residuals calculation is negligible.

The fitting procedure optimization defined the final fit function used for the data analysis of the single cell spectra. Figure 5 reports, as an example, the residual distribution for four additional single cells coupled with their dedicated Front-End electronics. The system linearity is confirmed to be at the level of few electronvolts, with residuals distributed around zero as in the previous case.

Given the  $\Delta E/E < 10^{-3}$  linear response of the SDDs system, the calibrated spectra of the SDDs with comparable statistics have been summed up to test the collective effects on the global response for a set made by two individual

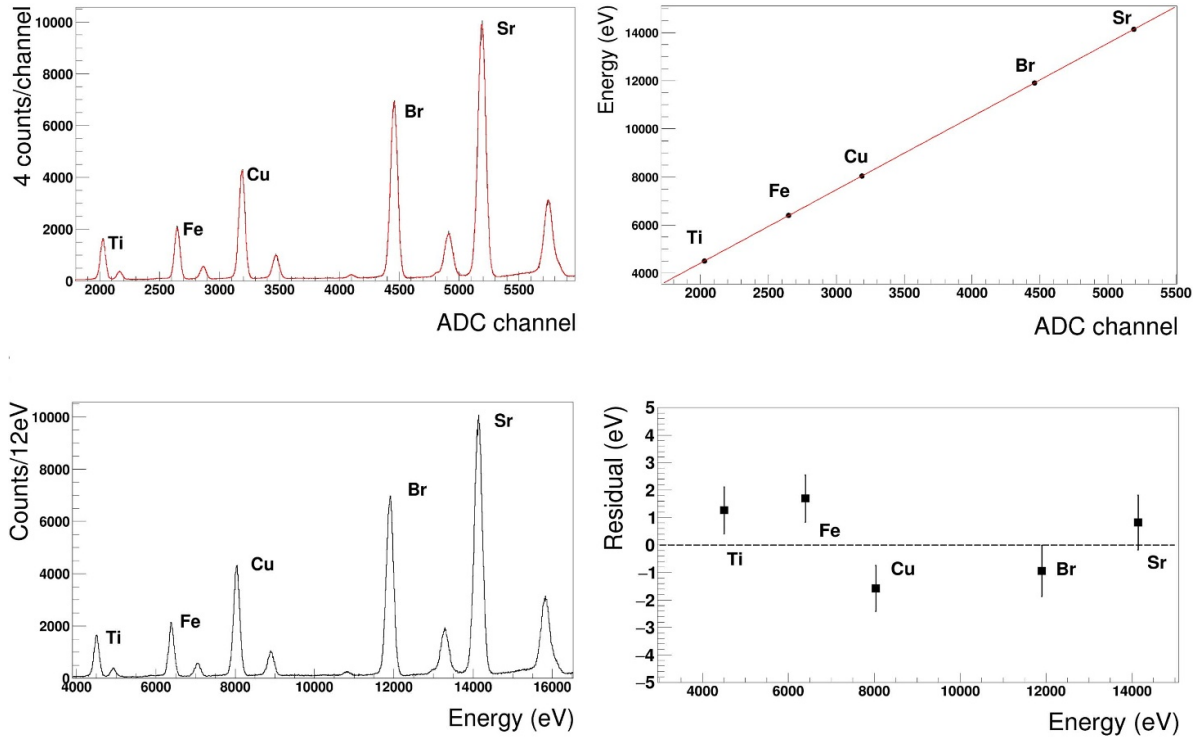


**Figure 4.** Typical example of a SDDs system unit energy response analysis. Top-left: Fit (red) in the energy range from 4000 eV to 16 000 eV. The reduced chi-square value of the fit is 1.8. Top-right: Calibration function to determine the ADC-to-eV conversion for the investigated cell. Bottom-left: Calibrated spectrum. Bottom-right: Plot of the residuals for single  $K_{\alpha}$  lines of the spectrum.

**Table 1.** Residual and systematic errors estimation for the SDDs system unit in figure 4. First column  $R_i$  values refers to the residuals of the 4 chs binning spectrum in figure 4.

Peak	$R_i$ eV	$R_i$ (2 chs bin) eV	$R_i$ (no rebin) eV	$R_i$ (Lin. bkg) eV	(+) Syst. error eV	(-) Syst. error eV
<i>Ti</i> $K_{\alpha}$	1.262	1.285	1.195	1.326	0.064	-0.067
<i>Fe</i> $K_{\alpha}$	1.689	1.676	1.677	1.691	0.002	-0.013
<i>Cu</i> $K_{\alpha}$	-1.576	-1.530	-1.514	-1.577	0.062	-0.001
<i>Br</i> $K_{\alpha}$	-0.944	-0.892	-0.931	-0.948	0.053	-0.003
<i>Sr</i> $K_{\alpha}$	0.818	0.782	0.807	0.837	0.019	-0.036

SDDs systems. In particular, the final spectrum obtained by the sum of 15 calibrated SDDs system units is shown in figure 6 left.

The higher statistics reveals the presence of impurity materials, such as the small Bi  $L_{\alpha}$  peak at 10 828 eV and Bi  $L_{\beta}$  peak at 13 008 eV, generated by the interaction of the beam products with the ceramic carrier of the SDDs array. However, they do not constitute a contamination concern for the experiment, being at the higher limit of the SIDDHARTA-2 ROI. No other impurity peaks are detected, confirming the purity of the experimental apparatus.

Figure 6 right reports the differences between the calibrated and the theoretical values for each  $K_{\alpha}$  peak. The deviation from the linearity is consistent with the previous estimation, mainly driven by the electronic chain, clinching the  $\Delta E/E < 10^{-3}$  global linearity of the system. Furthermore, the resolution of the Fe  $K_{\alpha}$  line is  $157.8 \pm 0.3^{+0.2}_{-0.2}$  eV, compatible with the typical low electronic noise SDDs employed for x-ray spectroscopy; systematic errors has been evaluated applying

the same variations as for residuals. No radiation damage has been observed during the tests.

Overall, figure 6 confirms that, even if the SDDs system is exposed to the ionizing background originated during the DAΦNE beam commissioning phase, the global energy response is linear ( $\Delta E/E < 10^{-3}$ ) with good energy resolution, matching the requirements to perform high-precision kaonic atoms spectroscopy measurements.

#### 4. Conclusions

The SDDs system developed by the SIDDHARTA-2 Collaboration has been tested for the first time at the DAΦNE collider of INFN-LNF. The crucial requirements needed to achieve the high-precision measurement of the (K-d) fundamental level, namely a linear energy response and a low electronic noise signal processing chain for the SDDs based detector system, have been evaluated during the DAΦNE beam commissioning phase, where the device exposition to the intense amount of

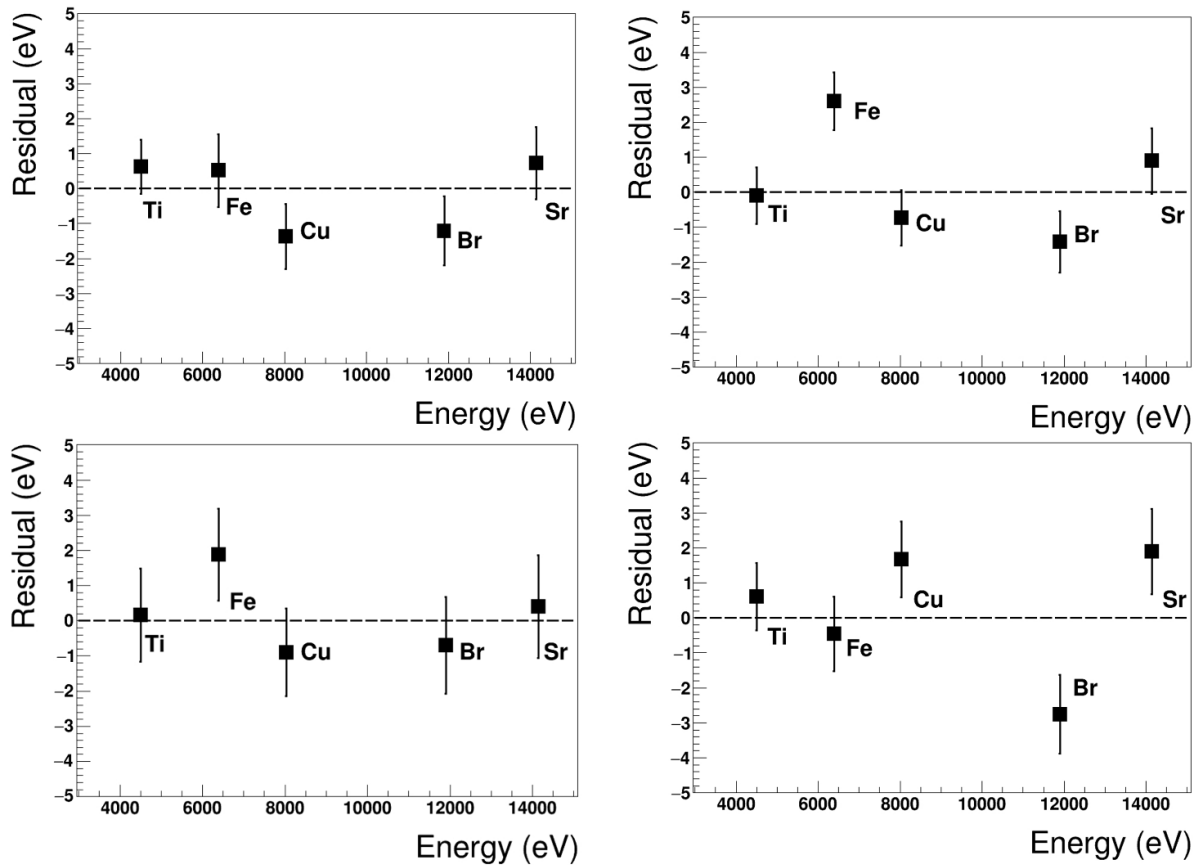


Figure 5. Residuals plots for four different SDDs system units.

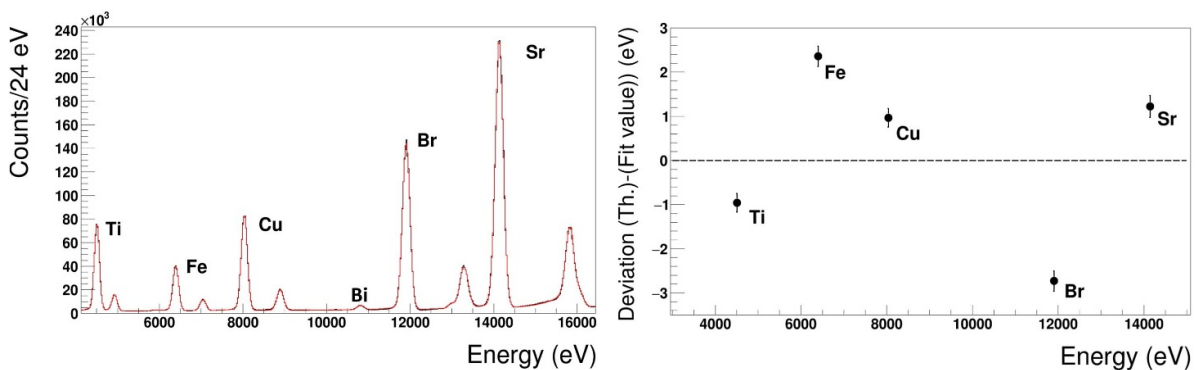


Figure 6. Left: Sum spectrum obtained by adding up 15 SDD calibrated spectra. Right: Residual plots for the  $K_{\alpha}$  peaks, obtained after the fit.

ionizing particles and radiation establishes a more stressful and realistic environment with respect to typical laboratory tests.

The ADC-to-eV calibration function, obtained after the fit procedure optimization, defines the SDDs system linearity of  $\Delta E/E < 10^{-3}$  showing residuals distributed within  $\pm 3$  eV. The solidity of the DAQ chain (analog and digital) has been tested by summing up 15 SDDs units, confirming a  $\Delta E/E < 10^{-3}$  global linearity and good energy resolution. The assessed linearity preservation both through the DAQ chain and in the high background conditions of the DAΦNE collider together with a measured energy resolution of  $157.8 \pm 0.3^{+0.2}_{-0.2}$  eV

(FWHM @ Fe  $K_{\alpha}$  line) at 170 K, proved SDDs system being a concrete solution and a natural choice not only for the SIDDHARTA-2 experiment, but more in general for all those applications and experiments requiring large area x-ray detectors for high-precision spectroscopy measurements able to work in challenging background conditions.

#### Data availability statement

The data that support the findings of this study are available upon reasonable request from the authors.

## Acknowledgments

We thank C Capoccia from LNF-INFN and H Schneider, L Stohwasser, and D Pristauz Telsnigg from Stefan-Meyer-Institut für Subatomare Physik for their fundamental contribution in designing and building the SIDDHARTA-2 setup. We thank as well the DAΦNE staff for the excellent working conditions and permanent support. Part of this work was supported by the Austrian Science Fund (FWF): [P24756-N20 and P33037-N]; the Croatian Science Foundation under the project IP-2018-01-8570; EU STRONG-2020 project (Grant Agreement No. 824093) and the Polish Ministry of Science and Higher Education Grant No. 7150/E-338/M/2018.

## ORCID iDs

M Miliucci  <https://orcid.org/0000-0002-2315-2379>  
 D Bosnar  <https://orcid.org/0000-0003-4784-393X>  
 R Del Grande  <https://orcid.org/0000-0002-7599-2716>

## References

- [1] Newbury D E and Ritchie N W M 2015 Performing elemental microanalysis with high accuracy and high precision by scanning electron microscopy/silicon drift detector energy-dispersive x-ray spectrometry (SEM/SDD-EDS) *J. Mater. Sci.* **50** 493–518
- [2] Campana R *et al* 2011 Imaging performance of a large-area silicon drift detector for x-ray astronomy *Nucl. Instrum. Methods Phys. Res. A* **633** 22–30
- [3] Bazzi M *et al* 2011 Performance of silicon-drift detectors in kaonic atom x-ray measurements *Nucl. Instrum. Methods Phys. Res. A* **628** 264–7
- [4] Fiorini C *et al* 2006 A large-area monolithic array of silicon drift detectors for medical imaging *Nucl. Instrum. Methods Phys. Res. A* **568** 96–100
- [5] Merafina M *et al* 2020 Self-gravitating strange dark matter halos around galaxies *Phys. Rev. D* **102** 083015
- [6] Curceanu C *et al* 2020 Kaonic atoms to investigate global symmetry breaking *Symmetry* **12** 547
- [7] Curceanu C *et al* 2019 The modern era of light kaonic atom experiments *Rev. Mod. Phys.* **91** 025006
- [8] De Pietri R *et al* 2019 Merger of compact stars in the two-families scenario *Astrophys. J.* **881** 122
- [9] Bazzi M *et al* 2011 A new measurement of kaonic hydrogen x-rays *Phys. Lett. B* **704** 113–7
- [10] Milardi C *et al* 2018 Preparation activity for the SIDDHARTA-2 run at DAΦNE IPAC-2018 **334–7**
- [11] Zobov M *et al* 2010 Test of ‘crab-waist’ collisions at the DAΦNE  $\Phi$  factory *Phys. Rev. Lett.* **104** 174801
- [12] Doring M and Meißner U G 2011 Kaon-nucleon scattering lengths from kaonic deuterium experiments revisited *Phys. Lett. B* **704** 663–6
- [13] Shevchenko N V 2012 Near-threshold K-d scattering and properties of kaonic deuterium *Nucl. Phys. A* **890–891** 50–62
- [14] Hoshino T S *et al* 2017 Constraining the  $\bar{K}N$  interaction from the 1S level shift of kaonic deuterium *Phys. Rev. C* **96** 045204
- [15] Bazzi M *et al* 2013 Preliminary study of kaonic deuterium x-rays by the SIDDHARTA experiment at DAΦNE *Nucl. Phys. A* **907** 69–77
- [16] Skurzok M *et al* 2020 Characterization of the SIDDHARTA-2 luminosity monitor *JINST* **15** 10010
- [17] Lechner P *et al* 1996 Silicon drift detectors for high resolution room temperature x-ray spectroscopy *Nucl. Instrum. Meth. Phys. Res. A* **377** 346–51
- [18] Lechner P *et al* 2001 Silicon drift detectors for high count rate x-ray spectroscopy at room temperature *Nucl. Instrum. Meth. Phys. Res. A* **458** 281–7
- [19] Lechner P *et al* 2004 Novel high-resolution silicon drift detectors *X-Ray Spectrom.* **33** 256–61
- [20] Miliucci M *et al* 2019 Energy response of silicon drift detectors for kaonic atom precision measurements *Condens. Matter* **4** 31
- [21] Bombelli L *et al* 2011 Low-noise CMOS charge preamplifier for x-ray spectroscopy detectors *IEEE Nucl. Sc. Symp. Conf. Record* **135–8**
- [22] Quaglia R *et al* 2016 Development of arrays of silicon drift detectors and readout ASIC for the SIDDHARTA experiment *Nucl. Instrum. Methods Phys. Res. A* **824** 449–51
- [23] Schembari F *et al* 2016 SFERA: an integrated circuit for the readout of x and  $\gamma$ -ray detectors *IEEE Trans. Nucl. Sci.* **63** 1797–807
- [24] Campbell J L 1990 X-ray spectrometers for PIXE *Nucl. Instrum. Methods Phys. Res. B* **49** 115–25
- [25] Campbell J L and Maxwell J A 1997 A cautionary note on the use of the hypermet tailing function in x-ray spectrometry with Si(Li) detectors *Nucl. Instrum. Methods Phys. Res. B* **129** 297–99
- [26] Van Gysel M, Lemberge P and Van Espen P 2003 Implementation of a spectrum fitting procedure using a robust peak model *X-Ray Spectrom.* **32** 434–41